Development of New Concepts for the Control of Polymerization Processes: Multiobjective Optimization and Decision Engineering. II. Application of a Choquet Integral to an Emulsion Copolymerization Process

Mauricio Camargo,[1] Laure Morel,[1] Christian Fonteix,[2] Sandrine Hoppe,[2] Guo-Hua Hu,[2] Jean Renaud[1]

[1]*Equipe de Recherche des Processus Innovatifs, Nancy-Université, EA 3767 8, rue Bastien Lepage, 54010 Nancy Cedex, France*
[2]*LRGP Laboratoire de la Réaction et le Génie de Procédés, ENSIC-INPL-CNRS, 1, Nancy-Université, rue Grandville, BP20451, 54001 Nancy Cedex, France*

Received 14 January 2009; accepted 2 September 2010
DOI 10.1002/app.33348
Published online 14 February 2011 in Wiley Online Library (wileyonlinelibrary.com).

ABSTRACT: In polymer industry, engineers seek to obtain polymers with prescribed end-use properties, high productivities, and low cost. Thus, the optimization of a manufacturing process with all those goals and constraints belongs to a problem domain that aims to achieve the best trade-off possible. This article concerns the optimization of the batch emulsion polymerization of styrene and α-methylstyrene. An accurate model was developed to describe the complete patterns of the emulsion polymerization. Key parameters of the model were identified on the basis of batch experimental data. The model was then used to simulate, under several operating conditions, the polymerization rate, the overall conversion of monomers, and the number and weight-average molecular weights. A multicriteria optimization approach based on an evolutionary algorithm and the concept of dominance from the Pareto frontier theory was used. Last, a decision aid system based on the Choquet integral was proposed to determine the optimal operating conditions with the preferences of the decision maker taken into account. © 2011 Wiley Periodicals, Inc. J Appl Polym Sci 120: 3421–3434, 2011

Key words: calculations; copolymerization; emulsion polymerization; kinetics (polym.); modeling

INTRODUCTION

Many optimization problems are often multiobjective decision problems. For example, one may have to simultaneously optimize the polymer production, the cost of the process, and the product quality. Under the given operating conditions, it is likely that not all of these objectives are optimal. Multiple objectives are normally related to each other through a linear or empirical combination to form a scalar objective function[2] or an empirical buildup.[3] Another method consists of optimizing a criterion while imposing constraints on all of the other ones.[4] These methods and others depend on the *a priori* decision maker's preferences. Decisions thus made could be biased because the decision maker may not have a complete view of the overall compromises.

Multicriteria optimization, in the Pareto's sense, is defined as the set of efficient solutions corresponding to those nondominated solutions in the z-dimensional objective space, called the *Pareto front*. Following the concept of Pareto dominance, a solution x is dominated by another one y for a set of criteria if, x is worse or equal than y for all the criteria, and strictly worse for, at least, one criterion.[5] Recently, several scientific studies have applied Pareto multicriteria optimization to polymerization processes[6–10] and other industrial applications.[11,12] In chemical engineering, only few researchers have used decision engineering tools to seek a particular solution, taking into account the preferences of the decision.[13–20] In this article, we address this issue, particularly in the field of polymer reaction engineering.

In our previous article,[16] an original two-step methodology was developed. This method allows one to combine both optimization and decision aid. The first step consists of taking into account the whole set of criteria, without *a priori*, to achieve a set of potential solutions by multicriteria optimization with an evolutionary algorithm. As a result, the resulting set of compromises could provide new knowledge, which would help the decision maker to adjust her or his preferences. In a second step,

Correspondence to: M. Camargo (mauricio.camargo@ensgsi.inpl-nancy.fr).

recommendations are made to the decision maker, from the ranking of compromises obtained thanks to a tool using the adjusted decision maker's preferences.

Most early studies in this field dealt with narrow Pareto domains (space of operating conditions).[7] In those cases, the choice of the best solution could be relatively simple. The wider the Pareto domain is, the more difficult the definition of the best solution can be. Then, there is a need to use multicriteria decision aid (MCDA) tools. An MCDA tool gives a graphical representation of the set of Pareto's optimal solutions and the relationship between the criteria performances, the operating conditions, and a solution's ranking. This results in a complete vision of the problem for the decision maker. This article is placed in this context.

In practice, many decision makers consider the set of criteria as independent of each other. For others, the criteria may interact with each other. These interactions could be modeled by the Choquet integral, a decision-making tool not yet used in chemical engineering. This is the third original contribution of this work.

The Choquet integral is based on the theory of fuzzy measures.[21] The use of the fuzzy measures in a multicriteria decision-making allows the modeling of interactions among criteria.[22] For example, when two criteria are positively (or negatively) correlated, the importance of the two combined should be less (or more) than the sum of the importance of each of them. Many authors have proposed the use of the Choquet integral to decision support systems in several industrial applications.[23,24] It is claimed to be an adequate substitute of the weighted average. We prefer this multicriteria technique for two main reasons: fuzzy measures take into account the criteria relevance (the decision maker's preferences) and interactions among them.

The objective of this article was to improve the two-step methodology through the introduction of the Choquet integral as a decision aid tool. As illustrated in subsequent sections, this approach was applied to the emulsion copolymerization of styrene (STY) and α-methylstyrene (AMS). Emulsion polymerization processes are common for latex production, particularly for paints, varnishes, inks, and adhesives. For these applications, the final product is characterized by the end-use properties, such as wet scrub resistance and filmification. These end-use properties are functions of properties such as the glass-transition temperature, molecular weight distribution and initial weight fraction of AMS (w_{AMS}) in the copolymer (F_1), and conversion (Volatile Organic Compound, VOC rate). The optimization of a set of properties is a multicriteria problem. In fact, the target goals to be reached can often be conflicting. As a result, the optimum set of properties cannot be achieved simultaneously.

EXPERIMENTAL

The experimental methods and tools that we used for the emulsion copolymerization of STY and AMS followed those used for the emulsion polymerization of STY.[16] The two monomers were first emulsified in water in the form of droplets by a surfactant agent (a mixture of Genapol and Texapon) under stirring. Potassium persulfate (KPS), a water-soluble initiator, was also added to the emulsion when the reaction medium was at the reaction temperature. The copolymerization was carried out in a 1-L glass reactor. During the polymerization, the reactor was closed, agitated, and thermostated. Latex samples were taken from the reactor at chosen time intervals. They were analyzed by

- Gravimetric analysis to determine the overall conversion of the monomers.
- Gas chromatography to evaluate the residual monomer content and, consequently, the composition of the formed copolymer.
- Gel permeation chromatography coupled with a differential refractometer and a multiangle laser light-scattering device to obtain the molecular weight distribution and the number-average molecular weight (M_n) and weight-average molecular weight (M_w) of the copolymer.
- Quasi-elastic light scattering to determine the latex average particle diameter (d_P) values.

PROCESS MODELING

Assumptions

The main assumptions made for the model were as follows:

- The diameters of the monomer droplets and those of the growing particles were monodisperse.
- Because of the relatively high hydrophobicity of the monomers, propagation, chain transfer to the monomer, and termination reactions in the aqueous phase were negligible.
- Transfer to polymer reactions was not taken into account.
- Coagulation between particles was negligible.
- The reactor was assumed to be isothermal and ideally mixed. It is well-known that the reactor is not isothermal at industrial scale.[25] Nevertheless, it was verified that under the polymerization conditions used in this study, the reactor was isothermal.

Emulsion polymerization is a complex process, and its mechanism is well-known.[26] In this study, instead of a single big complex model, several small models were developed. Each model was aimed at describing/predicting a specific characteristic of the state process. For that purpose, all of the statistic distributions were assumed to be independent. Theoretically, this assumption may not be valid. However, it largely simplified the problem without a loss of the predictability or the accuracy of the model. The previous assumptions led to the model described in Table II in ref. 15.

Reaction rates

Initiator decomposition

The rate of decomposition of the initiator in the aqueous phase is given by eq. (1):[16]

$$k_D(T) = k_{D0}(323.15\ \mathrm{K})\ \exp\left[-\frac{E_{ad}}{R}\left(\frac{1}{T}-\frac{1}{323.15}\right)\right] \quad (1)$$

where k_D is the thermal decomposition constant of the initiator in the aqueous phase, k_{D0} (323.15 K) is the thermal decomposition constant of the initiator in the aqueous phase at 323.15°K, T is the polymerization temperature, Ead is the activation energy, and R is the universal gas constant.

The free-radical efficiency in the aqueous phase (f) varied with the molar fraction of AMS in the monomer feed[27] (f_1) as follows:

$$f = f_0\ \exp(-bf_1) \quad (2)$$

where f_0 is the free-radical efficiency in the pure STY system and b is the initiator efficiency parameter.

Nucleation

The nucleation and surfactant partition were described in part I of this series.[16] The nucleation rate due to the presence of AMS is noted as R_{cm}. Because of the presence of AMS, the nucleation constant (k_{cm}) was calculated by

$$k_{cm} = \sum_{i=1}^{2} k_{cmi} f_{0i} \quad (3)$$

where f_{0i} is the initial molar fraction of monomer i in the reactor.

Rate of entry of radicals into particles

The capture rate of free radicals by particles (R_{cp}) depends on a kinetic parameter, as presented in part I of this series.[16]

Desorption

In part I, the desorption rate of free radicals was neglected. The results presented in ref. 28 show that the desorption rate of radicals that ended with an STY unit was 72 times lower than those of radicals that ended with an AMS unit. So, in this study, the desorption rate of free radicals terminated with an STY unit (R_2's) was neglected, whereas that terminated with an AMS moiety was taken in to account and was given by

$$R_{DS} = \frac{\delta_{\mathrm{des1}}}{d_p^2}\frac{N_P\bar{n}}{N_A}P_1 \quad (4)$$

where R_{DS} is the desorption rate of free radicals from particles, N_P is the number of particles, $\bar{n}$ is the average number of free radicals per particle, N_A is Avogadro's number (the number of molecules or particles in 1000 mol), and P_1 is the fraction of free radicals terminated with an AMS unit (R_1's) with regard to the total free radicals in the particle.

δ_{des1} is the desorption constant of R_1's and depends on

- Their diffusion coefficient in the aqueous phase.
- Their partition coefficient between the aqueous phase and the particles.[29]
- The fraction of desorbed free radicals. This depends on the monomer chain-transfer coefficient.[30]
- Their diffusion coefficient in the particles.[31]

The rate of desorbed free radicals entering the aqueous phase is fR_{DS}.[28] The factor f has the same value as that in eq. (2), as shown by the parametric identification in refs. 2 and 32.

Propagation

The rate of polymerization of monomer j with free radicals terminated with monomer i (R_{Pij}) is given by

$$R_{Pij} = k_{Pij}\left[\mathrm{M}_j\right]_P\frac{N_P\bar{n}P_i}{N_A} \quad (5)$$

where k_{Pij} is the propagation rate constant, $[M_j]_P$ is the molar concentration of monomer j in the particles, and P_i is the fraction of free radicals terminated with monomer i.

The temperature dependency of k_{Pij} can be written as follows:

$$k_{Pij}(T) = k_{Pij0}(323.15\ \mathrm{K})\ \exp\left[-\frac{E_{apij}}{R}\left(\frac{1}{T}-\frac{1}{323.15}\right)\right] \quad (6)$$

where E_{apij} is the activation energy, and k_{pij0} (323.15 K) is the propagation rate constant at 323.15°K. In the case of a propagation reaction with a primary radical (R_0) resulting from a capture process, one has

$$k_{P0j}=\sum_{i=1}^{2} f_{0i}k_{Pij} \tag{7}$$

This is due to the fact that this reaction has a real effect, as observed during the simulations, only at the beginning of the polymerization process. For the entire polymerization time, the sensitivity of the simulation results on this parameter's value was weak [eq. (7)].

The homopolymerization of AMS is very difficult because of its low reactivity and low ceiling temperature (61°C).[28,33] In this study, we assumed that the homopolymerization of AMS did not occur:

$$k_{\mathrm{P11}} = 0 \tag{8}$$

Thus, the overall propagation rate (R_P) was

$$R_P = R_{P01} + R_{P21} + \sum_{i=0}^{2} R_{Pi2} \tag{9}$$

where STY and AMS are designated as 2 and 1, respectively.

Termination

As in article I, the termination reactions were assumed to be instantaneous. This assumption corresponded to the classical zero–one conditions model.[34] Concomitantly, the gel and glass effects were neglected.

Glass effect

The glass effect equation used for the propagation was the one proposed in the literature.[30] k_{Pij} is related to the weight fraction of the polymer in the particles (w_P):

$$\begin{cases} k_{Pij} = k_{Pij0} & \text{if } w_P \le 0.8 \\ k_{Pij} = k_{Pij0}\exp(-a(w_P - 0.8)) & \text{if } w_P > 0.8 \end{cases} \tag{10}$$

where a is an adjustable parameter and is assumed to be the same for propagation constants, and k_{P0ij} is the value of $k_{Pij}(T)$ calculated by equation 6.

Transfer to monomer

The transfer rate of monomer j with free radicals terminated with monomer i ($R_{\mathrm{TR}ij}$) is

$$R_{\mathrm{TR}ij} = k_{\mathrm{TR}ij}\left[\mathrm{M}_j\right]_P \frac{N_P \bar{n} P_i}{N_A} \tag{11}$$

where $[\mathrm{M}_j]_P$ is the molar concentration of monomer j in the particles. The temperature dependency of the transfer rate constant of the monomer ($k_{\mathrm{TR}ij}$) follows:

$$k_{\mathrm{TR}ij}(T) = k_{\mathrm{TR}ij0}(323.15\ \mathrm{K}).\exp\left(-\frac{E_{atrij}}{R}\left(\frac{1}{T}-\frac{1}{323.15}\right)\right) \tag{12}$$

where E_{atrij} is the activation energy, and $k_{\mathrm{TR}ij0}$ (323.15 K) is the transfer rate constant of the monomer at 232.15°K. In the case of a transfer reaction of the monomer to R_0 resulting from the capture process, one has

$$k_{\mathrm{TR}0j} = \sum_{i=1}^{2} f_{0i}k_{\mathrm{TR}ij} \tag{13}$$

Then, the overall transfer rate (R_{TR}) can be defined as

$$R_{\mathrm{TR}} = \sum_{i=0}^{2}\sum_{j=1}^{2} R_{\mathrm{TR}ij} \tag{14}$$

Volume of each phase and the monomer partition

Calculation of volumes

The engaged volume of the polymerizing system in the reactor (V_R) is given by

$$V_R = V_{R0} + V_{\mathrm{AQ}}\sum_{i=1}^{2} M_{0i}X_iM_i\left(\frac{1}{\rho_{Pi}}-\frac{1}{\rho_i}\right) \tag{15}$$

where V_{R0} is the initial volume of the polymerizing system in the reactor, V_{AQ} is the volume of the aqueous phase (constant), M_{0i} is the initial concentration of monomer i (mol/aqueous phase volume), X_i is the total mass conversion of monomer i, M_i is the molecular weight of monomer i, ρ_{Pi} is the density of monomer i in the polymer, and ρ_i is the density of monomer i. The volume of the polymer (V_{POL}) is

$$V_{\mathrm{POL}} = V_{\mathrm{AQ}}\sum_{i=1}^{2} M_{0i}X_i\frac{M_i}{\rho_{Pi}} \tag{16}$$

The volume of the particles (V_P) and the volume of the droplets (V_D) are given by

$$\begin{cases} \text{if } V_R > V_{\mathrm{AQ}} + \frac{V_{\mathrm{POL}}}{1-\phi} \\ \text{then } V_P = \frac{V_{\mathrm{POL}}}{1-\phi} \text{ and } V_D = V_R - V_{\mathrm{AQ}} - V_P \\ \text{else } V_D = 0 \text{ and } V_P = V_R - V_{\mathrm{AQ}} \end{cases} \tag{17}$$

where ϕ is the volume fraction of monomers in the particles. d_P is given by

$$d_p = \sqrt[3]{\frac{6V_P}{\pi N_P V_{\mathrm{AQ}}}} \tag{18}$$

Mass and molecular fractions and concentrations

f_{0i} (in all monomers) is

$$f_{0i} = \frac{M_{0i}}{\sum_{j=1}^{2} M_{0j}} \tag{19}$$

where M_{0j} is the initial concentration of monomer j. The molar fraction of monomer i (f_i) is

$$f_i = \frac{M_{0i}(1 - X_i)}{\sum_{j=1}^{2} M_{0j}(1 - X_j)} \tag{20}$$

where X_j is the total mass conversion of monomer j.

The partition of the monomers in droplets and particles yields the following $[M_i]_P$:

$$[M_i]_P = \frac{f_i\left(1 - \frac{V_{\mathrm{POL}}}{V_P}\right)}{\sum_{j=1}^{2} f_j \frac{M_j}{\rho_j}} \tag{21}$$

where M_j is the molecular weight of monomer j and ρ_j is the density of monomer j.

w_P is given by

$$\frac{w_p}{1 - w_p} = \frac{V_{\mathrm{AQ}} \sum_{i=1}^{2} M_{0i} X_i M_i}{V_P \sum_{i=1}^{2} [M_i]_P M_i} \tag{22}$$

F_1 is

$$F_1 = \frac{M_{01} X_1}{X \sum_{i=1}^{2} M_{0i}} \tag{23}$$

where X is the overall conversion.

Balances

The balances of the initiator, free radicals, and N_P in the aqueous phase were the same as those presented in article I.

The balance of free radicals is

$$\frac{dR_w}{dt} = 2 f R_D - R_{cp} - R_{cm} + f R_{DS} \tag{24}$$

where R_w is the free radical concentration in the aqueous phase, and R_{DS} is an output rate for the particle phase. The input rate of radicals for the aqueous phase is fR_{DS}. f is the same factor as that corresponding to initiation because the phenomenon is the same.[28,32] It corresponds to the probability of the existence of radicals in the aqueous phase.

Balances of the monomers

The balance for AMS was as follows:

$$M_{01} \frac{dX_1}{dt} = R_{P01} + R_{P21} + R_{TR01} + R_{TR11} + R_{TR21} \tag{25}$$

The balance for STY was as follows:

$$M_{02} \frac{dX_2}{dt} = \sum_{i=0}^{2} R_{Pi2} + \sum_{i=0}^{2} R_{TRi2} \tag{26}$$

The balance of the total monomer was as follows:

$$\frac{dX}{dt} \sum_{i=1}^{2} M_{0i} = R_P + R_{TR} \tag{27}$$

Balances of the free radicals

There were three types of free radicals in the particles: R_0's (fraction P_0), R_1's (fraction P_1), and R_2's (fraction P_2).

The balance in R_1's was as follows:

$$\frac{d\left(\frac{N_P \overline{n} P_1}{N_A}\right)}{dt} = R_{P01} + R_{P21} - R_{P12} + R_{TR01} + R_{TR21} - R_{TR12} - R_{cp} \overline{n} P_1 - R_{DS} \tag{28}$$

The balance for R_2's was as follows:

$$\frac{d\left(\frac{N_P \overline{n} P_2}{N_A}\right)}{dt} = R_{P02} + R_{P12} - R_{P21} + R_{TR02} + R_{TR12} - R_{TR21} - R_{cp} \overline{n} P_2 \tag{29}$$

with $\sum_{i=0}^{2} P_i = 1$.

The total balance for free radicals was as follows:

$$\frac{d\left(\frac{N_P \overline{n}}{N_A}\right)}{dt} = R_{cm} + R_{cp}(1 - 2\overline{n}) - R_{DS} \tag{30}$$

Polymerization degree of the free radicals

The determination of the distribution moments was inspired by Villermaux,[35] who developed a method for modeling free-radical homogeneous polymerization

TABLE I
Selected Characteristics of the Monomers

Description	STY	AMS
Supplier	Aldrich (Lyon, France)	Fluka (Lyon, France)
Molecular weight (g/mol)	104.15	118.18
Density at 20°C (g/L)	906	908
Density of the homopolymer (g/L)	1070	1150

reactions. This method of moments was adapted here to determine the moments of the molecular weight distribution in the emulsion polymerization.

In the case of the macroradicals, the number of active chains corresponded to $N_P\overline{n}$. $\overline{\lambda_1}$ and $\overline{\lambda_2}$ denote the average numbers of AMS and STY moieties in those macroradicals, respectively. The balance for $\overline{\lambda_1}$ is given by

$$\frac{d\left(\frac{N_P\overline{n}\overline{\lambda_1}}{N_A}\right)}{dt} = \sum_{j=0}^{2} R_{TRj1} + R_{P01} + R_{P21} - (R_{TR} + R_{cp}\overline{n})\overline{\lambda_1} - R_{DS} \quad (31)$$

The balance for $\overline{\lambda_2}$ is given by

$$\frac{d\left(\frac{N_P\overline{n}\overline{\lambda_2}}{N_A}\right)}{dt} = \sum_{j=0}^{2} R_{TRj2} + \sum_{j=0}^{2} R_{Pj2} - (R_{TR} + R_{cp}\overline{n})\overline{\lambda_2} - R_{DS2} \quad (32)$$

Molecular weight distribution

The number of polymer chains (N_c) is the sum of number of active chains and the number of dead polymer molecules. The balance of chains is

$$\frac{d\left(\frac{N_c}{N_A}\right)}{dt} = R_{cm} + R_{TR} + R_{cp}(1 - \overline{n}) - R_{DS} \quad (33)$$

λ_1 and λ_2 denote the average numbers of AMS and STY moieties in all the polymer chains. The balance of λ_1 is given by

$$\frac{d\left(\frac{N_c\lambda_1}{N_A}\right)}{dt} = \sum_{j=0}^{2} R_{TRj1} + R_{P01} + R_{P21} - R_{DS} \quad (34)$$

The balance of λ_2 is given by

$$\frac{d\left(\frac{N_c\lambda_2}{N_A}\right)}{dt} = \sum_{j=0}^{2} R_{TRj2} + \sum_{j=0}^{2} R_{Pj2} \quad (35)$$

M_n is calculated by

$$M_n = \sum_{i=1}^{2} M_i\lambda_i \quad (36)$$

To calculate M_w, it is necessary to determine several second moments of the degree of polymerization. μ_1, μ_2, and μ are the second moments of the number of AMS moieties, STY moieties, and the sum of both in the polymer chains, respectively. The corresponding balances are

$$\frac{d\left(\frac{N_c\mu_1}{N_A}\right)}{dt} = \sum_{j=0}^{2} R_{TRj1} + R_{P01} + R_{P21}\left(1 + 2\overline{\lambda_1}\right) - R_{DS1} \quad (37)$$

$$\frac{d\left(\frac{N_c\mu_2}{N_A}\right)}{dt} = \sum_{j=0}^{2} R_{TRj2} + R_{P01} + \left(1 + 2\overline{\lambda_2}\right)\sum_{j=1}^{2} R_{Pj2} - R_{DS2} \quad (38)$$

$$\frac{d\left(\frac{N_c\mu}{N_A}\right)}{dt} = R_{TR} + \sum_{j=0}^{2} R_{P0j} + \left(R_{P21} + \sum_{j=1}^{2} R_{Pj2}\right) \times \left(1 + 2\left(\overline{\lambda_1} + \overline{\lambda_2}\right)\right) - R_{DS} \quad (39)$$

The variances of the numbers of AMS and STY moieties in the chains were $\mu_1 - \lambda_1^2$ and $\mu_2 - \lambda_2^2$, respectively. The covariance of the moments for the number of monomer moieties is given by $\nu - \lambda_1\lambda_2$ with

$$\mu = \mu_1 + \mu_2 + 2\upsilon \quad (40)$$

M_w is given by

$$M_nM_w = M_1^2\mu_1 + M_2^2\mu_2 + 2M_1M_2\upsilon \quad (41)$$

The combination of eqs. (40) and (41) leads to

$$M_2 = \frac{M_1M_2\mu + (M_1 - M_2)(M_1\mu_1 - M_2\mu_2)}{M_n} \quad (42)$$

ESTIMATION OF THE MODEL PARAMETERS

Data for parametric identification

The goal of this model was to predict the monomer conversions, M_n, M_w, N_P per unit of volume of the aqueous phase, d_P values, and concentrations as a function of time for different process operating conditions, such as temperature, surfactant, initial concentration of the initiator ($[A]_0$), and initial concentrations of the monomers ($[M]_0$'s).

TABLE II
Values of Properties from the Literature

Temperature (°C)	S_{cmc} (g/L)[41]	ϕ[42]
50	2.0	
65	2.2	0.6
85	2.3	

Table I shows selected characteristics of the monomers.[36] The value of the density of poly(α-methylstyrene) corresponded to an estimated property of an AMS moiety in a polymer chain.

The copolymerization of AMS and STY was different from the homopolymerization of STY reported in part I of this series.[16] Moreover, the surfactant was not sodium dodecyl sulfate but a mixture of Texapon and Genapol. Nevertheless, the parameters of the homopolymerization in part I[16] were used for the copolymerization.

The energies of activation for the persulfate decomposition, propagation, and monomer transfer were 135, 32.5, and 55.9 kcal/mol, respectively.[27] The other parameters were temperature dependent, but their variations were considered to be negligible.

Polymerization experiments without AMS (the homopolymerization of STY) were carried out at 50, 65, and 85°C, respectively. The total $[M]_0$ was 2.184 mol/L. The total number of measurements was 61 for X, 46 for N_P per liter, and 17 for both M_n and M_w. No significant differences between the simulations and experimental data were found.

Identification of the kinetic parameters of the copolymerization was carried out with the model and values of the homopolymerization of STY described previously and those given in the literature.[34] Values for the critical concentration of the surfactant (S_{cmc}) and ϕ were the same as those for the homopolymerization of STY and were also used for the copolymerization of STY and AMS (Table II). Experiments were carried out in a 1-L closed reactor with water, KPS, STY, AMS, and a surfactant mixture composed of Texapon (T) and Genapol (D). The initial concentrations of these materials were as follows:

$$[\mathrm{KPS}]_0 = 1\,\mathrm{g/L} = 3.7 \times 10^{-3}\,\mathrm{mol/L} \quad (43)$$

$$[\mathrm{G}]_0 + [\mathrm{T}]_0 = 3S_{cmc} = 6.648\ \mathrm{g/L} \quad (44)$$

$$[\mathrm{G}]_0/[\mathrm{T}]_0 = 2 \quad (45)$$

Table III shows information on the copolymerization experiment. The total number of measurements were 261 for X, 221 for N_P per liter, 70 for both M_n and M_w, and 68 for F_1 [eq. (32)].

STY copolymerization

The parameters were determined by optimization of the maximum likelihood criteria[37] from the experimental data. Identification of b allowed us to reduce the initiator efficiency as a function of the residual concentration of AMS. The presence of the AMS reduced the initiator efficiency to a level of about 0.01. The gap between the experimental measurements and the model was higher than 100% at the beginning of the polymerization process. This last finding confirmed the theory[27] that the initiator efficiency depends on the nature of the monomers.

Identification of the propagation constants allowed us to determine the reactivity ratio (r_{12}). At 50°C, it was 1.1; this matched those of the literature, which range from 0.9 to 1.3.[38] The second r_{12} could not be calculated because, under the specified copolymerization conditions, the depropagation rate of AMS was very high compared with the propagation rate. The values reported in the literature are generally lower than 0.6;[38] this implied that the propagation constant of AMS (k_{P011}) would be very small. The activation energies for the propagation constant allowed us to calculate the r_{12} values at different temperatures: $r_{12} = 1.2$ at 65°C and $r_{12} = 1.3$ at 85°C.

The nucleation constant of AMS was higher than that of STY; this proved that N_P depended on the concentration of AMS in the system. In fact, the d_P values decreased with increasing initial concentration of AMS.

R_1's tend to desorb out of the particle.[39] $\bar{n}$ becomes lower than 0.5. Thus, the copolymerization of STY and AMS was different from the homopolymerization of STY (Table IV).

As mentioned in a previous section, four experiments were carried out at 50, 65, and 85°C. Fifteen figures were needed to show the conversion, particle number, M_n, M_w, and F_1. To reduce this number, we chose to show all of the variable evolutions at 50°C. One figure at 85°C completes these presented results.

Figure 1 shows the effect of the temperature on the evolution of the experimental and simulated

TABLE III
Copolymerization Experiments

Temperature (°C)	Total initial monomer concentration (mol/L)	w_{AMS}
50	2.159	0.089
50	2.120	0.227
50	2.094	0.322
50	2.055	0.468
65	2.159	0.089
65	2.120	0.227
65	2.094	0.322
65	2.055	0.468
85	2.159	0.089
85	2.120	0.227
85	2.094	0.322
85	2.055	0.468

TABLE IV
Optimal Values of the Parameters for the Copolymerization Model

Parameter	Meaning	Value
A	Glass effect coefficient	6.3
b	Initiator efficiency parameter	7.4
k_{P120}	Propagation constant AMS/STY at 50°C	41 L mol^{-1} s^{-1}
k_{P210}	Propagation constant STY/AMS at 50°C	273 L mol^{-1} s^{-1}
k_{TR110}	Monomer transfer constant AMS/AMS at 50°C	1.51×10^{-2} L mol^{-1} s^{-1}
k_{TR120}	Monomer transfer constant AMS/STY at 50°C	4.1×10^{-3} L mol^{-1} s^{-1}
k_{P210}	Monomer transfer constant STY/AMS at 50°C	2.09×10^{-2} L mol^{-1} s^{-1}
k_{cm1}	Nucleation constant of AMS	1.03×10^{-2} L g^{-1} s^{-1}
δ_{des1}	Desorption constant of R_1's	3.0×10^{-16} dm^2/s
E_{ap12}	Propagation activation energy of AMS/STY	15,500 J/mol
E_{ap21}	Propagation activation energy of STY/AMS	28,700 J/mol
E_{atr11}	Transfer activation energy of AMS/AMS	65,900 J/mol
E_{atr12}	Transfer activation energy of AMS/STY	117,700 J/mol
E_{atr21}	Transfer activation energy of STY/AMS	69,100 J/mol

conversions as a function of time in the case of the STY copolymerization with $w_{AMS} = 0.1$. As expected, an increase in the temperature led an increase in the polymerization rate. This effect existed also for the other w_{AMS}'s used (0.25, 0.35, and 0.5). Furthermore, the polymerization rate decreased with increasing w_{AMS}; this confirmed the low reactivity of AMS and its high tendency toward depropagation. Not all results used for modeling are presented here to limit the number of figures.

Figure 2 shows the experimental and simulated numbers of particles at 65°C during time for the different w_{AMS}'s. At each temperature, for times above 10,000 s, the experimental N_P increased with w_{AMS} until $w_{AMS} \in [0.25, 0.35]$ and then decreased as w_{AMS} increased. Under these conditions, the experimental N_P varied between 2.23×10^{17} and 3.68×10^{17} at 50°C, 4.37×10^{17} and 5.03×10^{17} at 65°C, and 6.38×10^{17} and 11.4×10^{17} at 85°C. However, the measurement error was nonnegligible. We do not have an explanation at this time for this phenomenon.

The model behavior is then even more complicated. At 50°C, for times up to 10,000 s, the simulated N_P decreased with increasing w_{AMS}. At 85°C, it increased continuously with increasing w_{AMS}. At 65°C (Fig. 2), the simulated N_P decreased with increasing w_{AMS} from 0.10 to 0.25 and increased with w_{AMS} from 0.25 to 0.50. The simulated N_P varied from 2.48×10^{17} to 3.97×10^{17} at 50°C, from 4.69×10^{17} to 5.11×10^{17} at 65°C, and from 7.22×10^{17} to 9.57×10^{17} at 85°C. For these three different

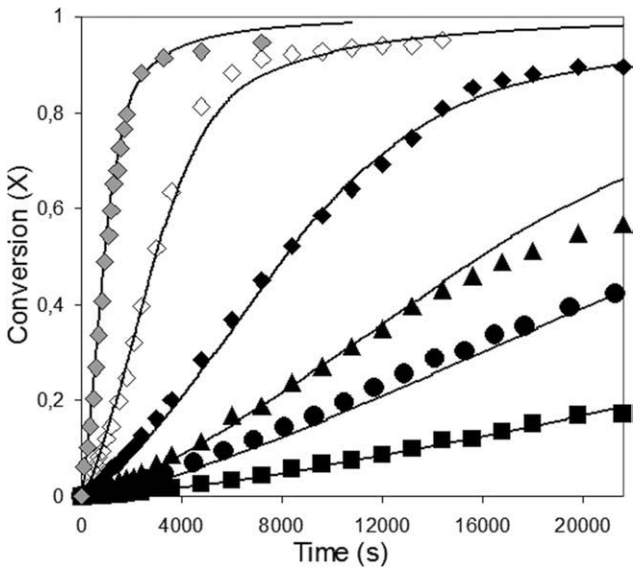

Figure 1 Effects of the temperature and w_{AMS} on the evolution of the experimental and simulated conversions over time: $T = 50$°C: $w_{AMS} = (\blacklozenge)$ 0.1 and $(\blacktriangle)$ 0.25, $(\bullet)$ 0.35, $(\blacksquare)$ 0.50; $(\diamond)$ $T = 65$°C and $w_{AMS} = 0.1$; and $(\diamond)$ $T = 80$ and $w_{AMS} = 0.1$

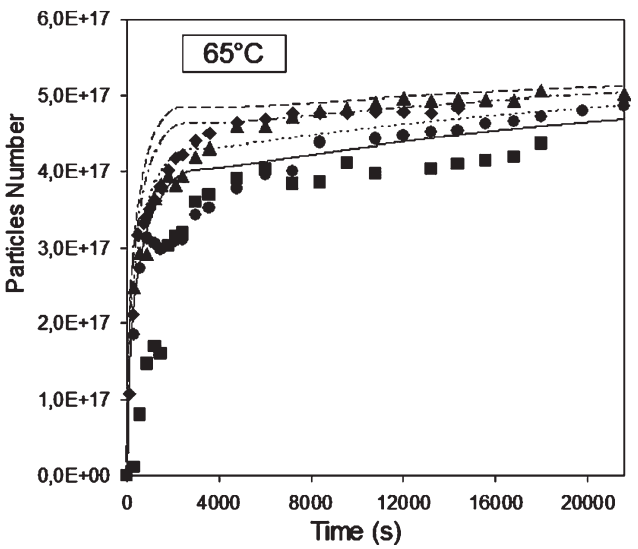

Figure 2 Comparison of the experimental and simulated N_P values at 65°C for different w_{AMS}'s: [$(\blacklozenge)$ experimental and (----) simulated] 0.1, $(\blacktriangle$ and —) 0.25, $(\bullet$ and . . .) 0.35, and $(\bullet$ and - - -) 0.50.

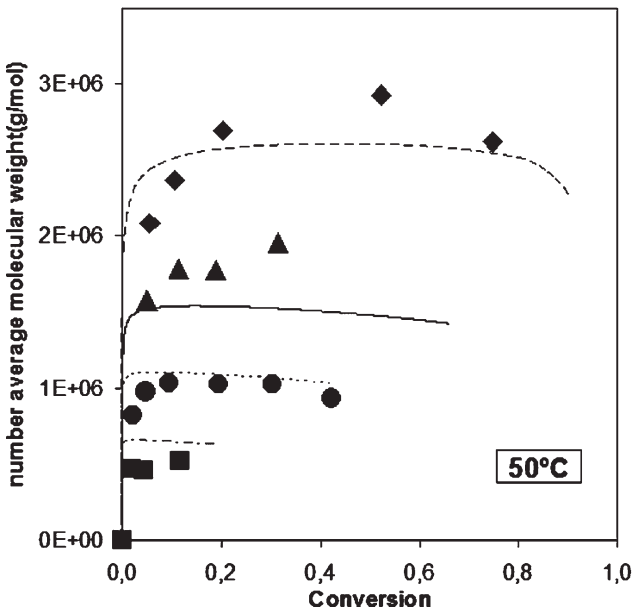

Figure 3 Comparison of the experimental and simulated M_n's at 50°C for different w_{AMS}'s: [(◆) experimental and (----) simulated] 0.1, (▲ and —) 0.25, (● and . . .) 0.35, and (● and - - -) 0.50.

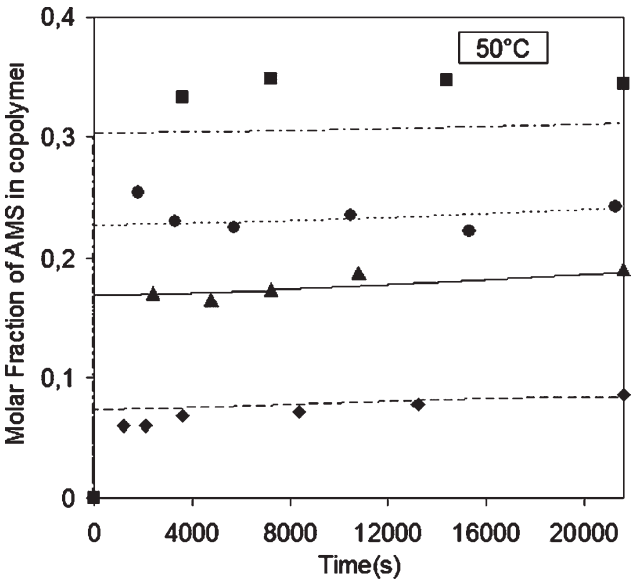

Figure 5 Comparison of the experimental and simulated F_1 values at 50°C and with different w_{AMS}'s: [(◆) experimental and (----) simulated] 0.1, (▲ and —) 0.25, (● and . . .) 0.35, and (● and - - -) 0.50.

temperatures, the evolution of N_P did not follow the same trend. Nevertheless, for each temperature, the ranges of variation were the same for the experiments and the simulations. On the other hand, the simulated and experimental N_P values increased with increasing temperature, whatever w_{AMS} was. As shown in Figure 2, at 65°C, both ranges of variation were narrow. The differences between the experimental and simulated data were within experimental error and the limits of the model and were small enough for the modeling purposes.

Figure 3 compares the experimental and simulated M_n values of the copolymer for different w_{AMS}'s at 50°C. The agreement was good. However, it was much worse when T was 65 or 85°C. This was related to the low ceiling temperature for the homopolymerization of AMS (61°C). The molecular mass

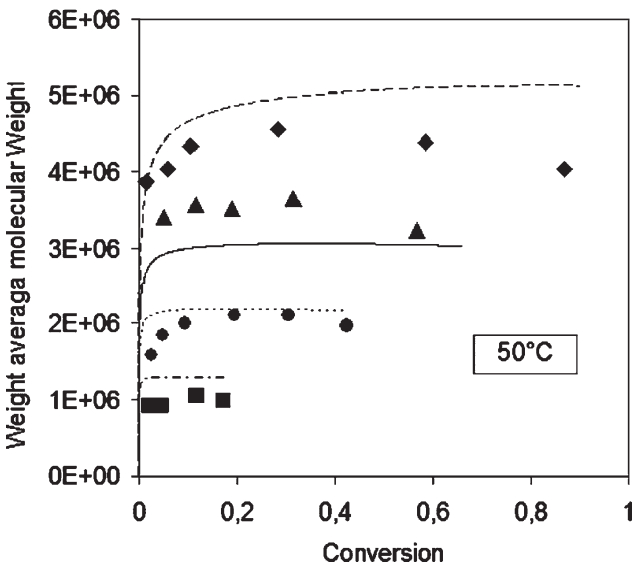

Figure 4 Comparison of the experimental and simulated M_w's at 50°C for different w_{AMS}'s: [(◆) experimental and (----) simulated] 0.1, (▲ and —) 0.25, (● and . . .) 0.35, and (● and - - -) 0.50.

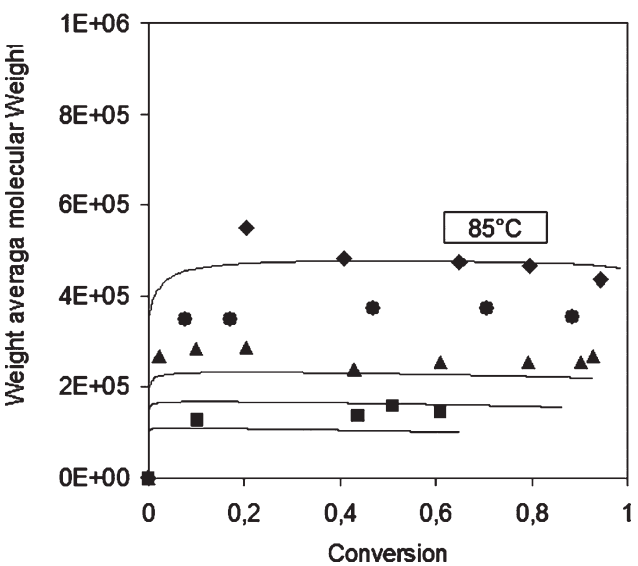

Figure 6 Comparison of the experimental and simulated M_w's at 85°C for different w_{AMS}'s: [(◆) experimental and (----) simulated] 0.1, (▲ and —) 0.25, (● and . . .) 0.35, and (● and - - -) 0.50.

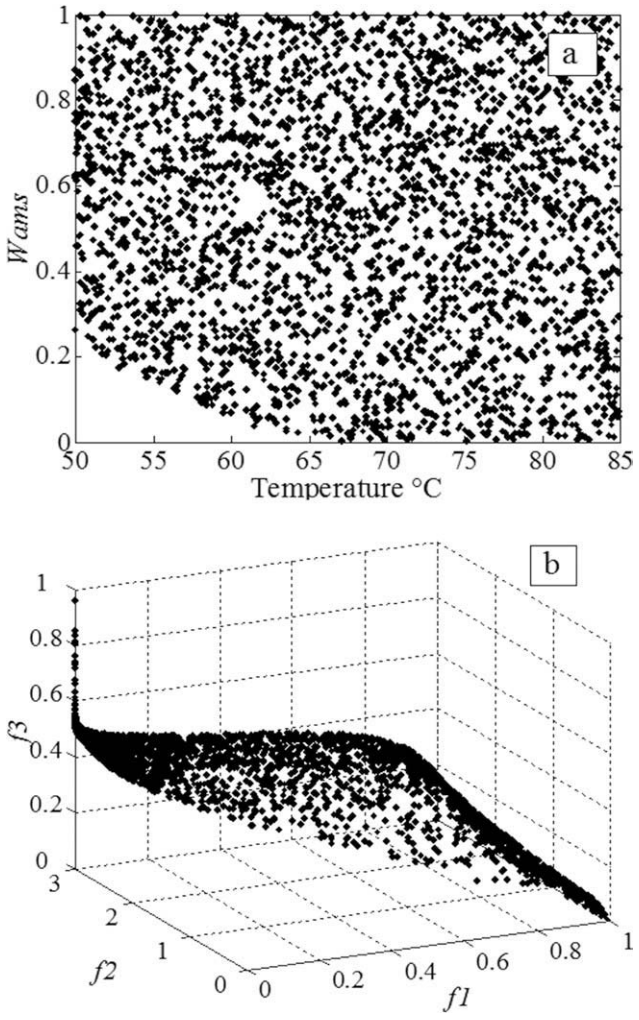

Figure 7 (a) Pareto zone and (b) Pareto front for the emulsion copolymerization of STY and AMS.

distribution was measured with STY homopolymer standards. Figure 4 compares the experimental and simulated M_n and M_w values at 50°C. Again the agreement was satisfactory. Similar results were obtained for the copolymerizations at 65 and 85°C. The experimental and simulated compositions of AMS in the copolymer were very close, whatever the copolymerization temperature was (50, 65, or 85°C). This is shown in Figures 5 and 6.

MULTICRITERIA OPTIMIZATION OF THE EMULSION COPOLYMERIZATION

Multicriteria optimization by an evolutionary algorithm

As indicated in the first section, the goal of this study was to determine a set of compromises corresponding to the Pareto optimal solutions (nondominated solutions). This is done by minimizing the number of times in which one solution is dominated by another.[40] Evolutionary algorithms are well adapted to multiobjective problems when an industrial process optimization is needed.[41,42] The one used to converge into the set of elements that best fit the criteria is predefined thanks to the dominance principle as described by Halsall-Whitney and Thibault.[43]

Problem statement and Pareto front approach

The copolymerization model explained previously allowed us to predict, after a given final time t_f, X, N_P, M_w, M_n, and F_1. The initial operating conditions considered were $[A]_0$, $[M]_0$, the initial concentration of the surfactant ($[S]_0$), T, and w_{AMS}. In this study, only T and w_{AMS} were varied. The first set of criteria to be optimized was defined with respect to the output parameters of the copolymerization model.

The goal was to optimize the quality of the obtained latex in terms of the monomer conversion, M_w, and w_{AMS}. In other words, the monomer conversion [eq. (46)] was to be maximized:

$$f_1 = X(t_f) \tag{46}$$

where f_1 is objective function 1 (monomer conversion). The difference between the predicted M_w and the target weight-average molecular weight [M_{wd}; eq. (47)] was minimized:

$$f_2 = |M_w(t_f) - M_{wd}| \tag{47}$$

where f_2 is objective function 2 (quality in terms of average molecular weight):

$$M_{wd} = 3 \times 10^6 \text{ g/mol} \tag{48}$$

w_{AMS} incorporated in the copolymer was maximized so that the hardness of the copolymer would be the highest [eq. (49)]:

$$f_3 = F_1(t_f) \tag{49}$$

where f_3 is objective function 3 (AMS fraction incorporated in the copolymer). N_P was not optimized in this study because the model was believed to be unable to predict it accurately. The next step was then to simultaneously optimize the three criteria (f_1, f_2, and f_3) with respect to two variables (T and w_{AMS}) under the following conditions:

$$50.15 \leq T \leq 85.15^{\circ}C \tag{50}$$

$$0 \leq w_{AMS} \leq 1 \tag{51}$$

$$[A]_0 = 3.7 \times 10^{-3} \text{mol/L} \tag{52}$$

$$[M]_0 = 2.184 \text{ mol/L} \tag{53}$$

TABLE V
Fuzzy interactions values

Fuzzy measure
$\mu_1 = \mu_2 = \mu_3 = 0.5$
$\mu_{12} = \mu_{21} = 0.9$
$\mu_{13} = \mu_{23} = 0.6$
$\mu_{31} = \mu_{32} = 0.8$

$$S_0 = 3S_{cmc} \tag{54}$$

$$t_f = 21,600 \text{ s} \tag{55}$$

The multicriteria optimization approach and the model developed in this study were then applied to the emulsion copolymerization of STY and AMS described previously. Figure 7(a) shows the Pareto zone (space of variables). As shown, almost the entire space was feasible. Figure 7(b) shows the Pareto front (space of criteria) that visualized the response surface of this phenomenon in a three-dimensional space. Obviously, it was difficult to simultaneously maximize f_1 and f_3 and minimize f_2.

Each point of the Pareto front corresponds to one point of the Pareto zone. Thus, one can choose one point of the Pareto front corresponding to her or his preferred product characteristics and then determine the corresponding operating conditions in the Pareto zone. However, making a choice is not easy and generally needs a decision support system.

The Pareto zone was too broad for this emulsion copolymerization system. In such a case, the use of a decision support system will help one choose the optimal operating conditions. An MCDA is a preference model capable of reproducing decision-maker preferences. It provides recommendations about the solutions in the Pareto front and their corresponding operating conditions.

Decision aid shell based on the Choquet integral

As mentioned,[44] the multicriteria model is composed of three main components:

- Formalism of criteria. This is implemented thanks to the utility functions and allows the establishment of the index measure between the criteria.
- Fuzzy measure. This is a set function that is set up to model the importance of the interactions between criteria.
- Choquet integral. This allows overall evaluation on calculation of an average value of the utilities with the importance of interactions between the criteria taken into account.

The Choquet integral was introduced by Choquet[21] on the basis of the theory of fuzzy measures. In comparison with other multicriteria analysis techniques, the Choquet integral has the following two characteristics:

- It extends the weighted approach of other techniques to a fuzzy set of criteria by taking into account interactions between them.
- It allows an expression of the degree of importance of a combination of criteria in a unique index.

The use of the fuzzy measures in a multicriteria decision-making enables the modeling of interactions among criteria.[23] For example, when two criteria are positively correlated, the importance of these criteria taken together should be strictly less (or more) than the sum of the importance of each of the single criteria.

The approach of aggregating scores to calculate an overall score is the basis of the multiattribute theory because scores on criteria are nothing other than utility values of attributes.[44] The aim of the multiattribute utility approach is to assign an overall score to each vector of scores when one takes into account the different criteria describing the preferences of the decision maker when considering several criteria simultaneously. The mechanism of the decision maker could be described by two components.[44] The *intracriteria preference* describes to the degree to which the values of a given attribute are satisfactory for the decision maker. In our case, this preference was indicated by the decision maker itself. The *intercriteria performance* describes to the degree to which coalitions and interactions of the criteria are important for the decision.

A fuzzy measure (μ) is defined under X. As an application, μ: $P(X) \rightarrow [0,1]$, which satisfies

$$\mu(X) = 1 \tag{56}$$

$$\mu(\phi) = 0 \tag{57}$$

where $P(X)$ is a set included in X, and (monotonicity)

$$S \subset T \subseteq X \Rightarrow \mu(S) \leq \mu(T) \tag{58}$$

where S and T are sets included in X. Finally, the aggregation function allows the overall evaluation of a solution. In this study, we used the Choquet integral to calculate an average value of the utilities, taking into account the interaction and the importance of the criteria.

The set of criteria (g_i) $X = \{g_1, g_2, \ldots g_n\}$ was evaluated with a set of utility functions (u_i). The result for a product P is $P_u = \{u_1, u_2, \ldots u_n\}$. Given $\mu(X)$, the overall evaluation index (GEI) of product A is as follows:

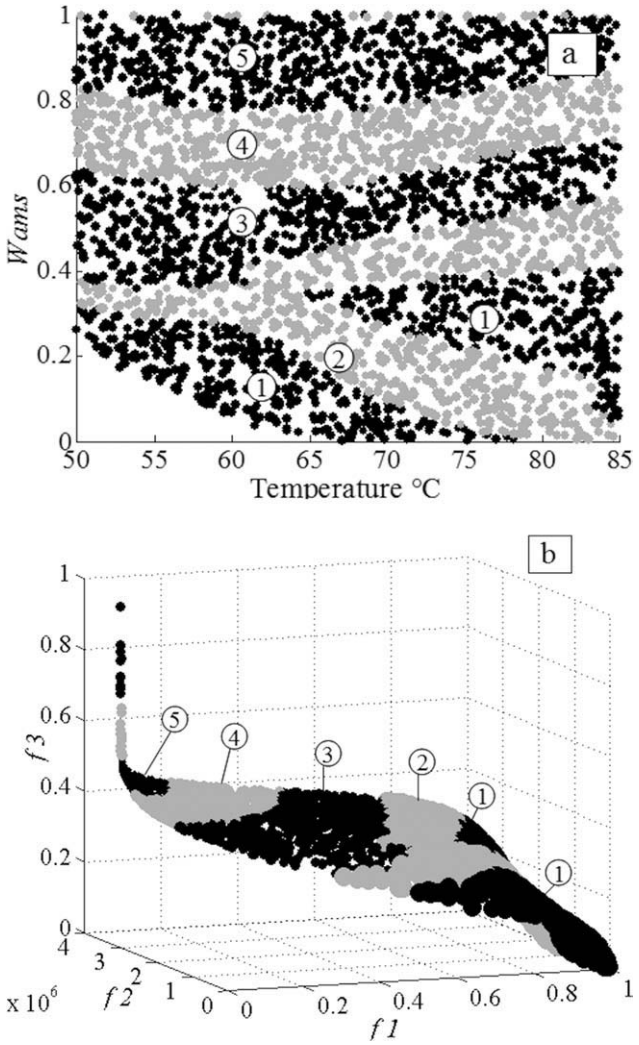

Figure 8 Ranking for 20% intervals of the (a) Pareto zone and (b) Pareto front.

$$\mathrm{GEI} = C_\mu(u_1, \ldots, u_n) = \sum_{i=1}^{n} (u_{(\sigma i)} - u_{(\sigma i-1)})\mu(A_{\sigma i}) \quad (59)$$

where $C_\mu(u_1,\ldots,u_n)$ is the Choquet integral and σ is an index permutation $1,\ldots,n$. In fact it is a range (u_i) in an increasing order:

$$0 = u_{\sigma 0} \le u_{\sigma 1} \le \cdots \le u_{\sigma n} \le 1 \text{ with } u_{\sigma 1} = \mathrm{Min}_{(i)ui} \text{ and } u_{\sigma n} = \mathrm{Max}_{(i)ui} \quad (60)$$

where $A_{\sigma i}$ represents a set of criteria defined by $A_{\sigma i} = \{g_{\sigma i},\ldots,g_{\sigma n}\}$.

This approach makes it possible to take into account experimental observations and expert know-how concerning the product itself and the manufacturing process to determine and evaluate interactions between variables. In this study, all of the criteria were considered to have the same importance and criteria f_1 and f_2 were considered to have higher interactions (Table V).

Criterion f_1, the maximization of the monomer conversion, and criterion f_2, the minimization of the difference between M_w and M_{wd}, are common to any type of latex. However, criterion f_3, the maximization of w_{AMS} incorporated in the copolymer, was specific to this emulsion copolymerization system. Therefore, any interaction with it was important when f_3 had the higher performance (μ_{31},μ_{32}). The operating conditions were ranked by GEI, which allowed us to identify the most promising regions of the Pareto zone (Fig. 8).

The region of solutions marked by number 1 indicates the preferred 20% of the solutions, those marked by number 2 indicate the following 20%, and those marked by number 5 correspond to the worst 20%. Comparison of the experimental data in Table III with the simulated ones in Figure 8 showed that among the 12 experiments for parametric identification, 6 were in zone 1. This indicated that the model was accurate within this zone and that this zone was well defined. Interestingly, region 1 was split into two zones. This implied that it could be possible to carry out the copolymerization at a high temperature and high w_{AMS} to obtain a copolymer with a high f_3. w_{AMS} in the resulting copolymer was about 30%. Nevertheless, this high w_{AMS} in the copolymer was at the expense of a low conversion (f_1) and a large gap between the predicted M_w and M_{wd} (f_2). On the other hand, a low temperature and low w_{AMS} led to a high f_1 and a low f_2. w_{AMS} in the copolymer (f_3) was low, too. These apparently contradictory solutions may give equal satisfaction or no satisfaction to a decision maker.

CONCLUSIONS

In this study, we aimed to develop a methodology to deal with optimization problems and multicriteria decisions for a batch emulsion copolymerization process. This was based on modeling, optimization, and decision-making tools to treat the entire set of information about the copolymerization. In particular, the multicriteria decision problem could be stated as follows: how could we define optimal process conditions so that the resulting product possessed a prescribed quality? The solution to it was to optimize several criteria simultaneously, even when some or all of them were conflicting. The results show that the use of the Pareto front optimization was not always sufficient to select the optimal operating conditions. The use of a decision aid system based on fuzzy measures, in particular, the Choquet integral, allowed us to identify the best solution for the decision maker. Decision engineering

provided valuable additional information for the multicriteria optimization of the polymerization processes.

NOMENCLATURE

Reaction rates

R_{cm}	nucleation rate due to the presence of AMS (kmol/s)
R_{cp}	capture rate of free radicals by particles
R_{DS}	desorption rate of free radicals from particles (kmol/s)
R_{Pij}	rate of polymerization of monomer j with free radicals terminated with monomer i
R_{TR}	overall transfer rate
$R_{\mathrm{TR}ij}$	transfer rate of monomer j with free radicals terminated with monomer i

Kinetic constants

δ_{des1}	desorption constant of the free radicals terminated with an AMS unit
k_{cm}	nucleation constant
k_D	thermal decomposition constant of the initiator in the aqueous phase (s^{-1})
f	free-radical efficiency in the aqueous phase
f_0	free-radical efficiency in the pure STY system
f_i	molar fraction of monomer i
k_{Pij}	propagation rate constant
$k_{\mathrm{TR}ij}$	transfer rate constant of the monomer
$\overline{n}$	average number of free radicals per particle

Product quantities

$[\mathrm{A}]_0$	initial concentration of the initiator
f_{0i}	initial molar fraction of monomer i in the reactor
f_1	molar fraction of AMS in the monomer feed
F_1	molar fraction of AMS in the copolymer
$\overline{\lambda_1}$	average number of AMS units per free radical
$\overline{\lambda_2}$	average number of STY units per free radical
λ_1	average number of AMS units per polymer chain
λ_2	average number of STY units per polymer chain
M_{0i}	initial concentration of monomer i
M_{0j}	initial concentration of monomer j
$[\mathrm{M}]_0$	initial concentration of the monomer
$[\mathrm{M}_i]_P$	molar concentration of monomer i in the particles
$[\mathrm{M}_j]_P$	molar concentration of monomer j in the particles
N_P	number of particles
P_0	fraction of primary free radicals
P_1	fraction of free radicals terminated with an AMS unit
P_2	fraction of free radicals terminated with an STY unit
P_i	fraction of free radicals terminated with monomer i
R_0	primary free radical (fraction P_0)
R_w	free radical concentration in the aqueous phase
r_{12}	reactivity ratio
R_1	free radical terminated with an AMS unit (fraction P_1)
R_2	free radical terminated with an STY unit (fraction P_2)
R_p	overall propagation rate
$[\mathrm{S}]_0$	initial concentration of the surfactant
tf	final time of polymerization
w_{AMS}	initial weight fraction of AMS
w_P	weight fraction of the polymer in the particles
X	overall conversion
X_i	total mass conversion of monomer i
X_j	total mass conversion of monomer j

Products properties

d_P	average particle diameter (m)
E_{ad}, E_{apij}, E_{atrij}	activation energy
μ	sum of μ_1 and μ_2
μ_1	second moment of the number of AMS moieties
μ_2	second moment of the number of STY moieties
M_n	number-average molecular weight (kg/kmol)
M_w	weight-average molecular weight (kg/kmol)
M_{wd}	target weight-average molecular weight (kg/kmol)
ν	covariance of the moments for the number of monomer moieties
N_c	number of polymer chains
ϕ	volume fraction of monomer in the particles
S_{cmc}	critical concentration of the surfactant
T	polymerization temperature

Others

b	initiator efficiency parameter
N_A	Avogadro's number (the number of molecules or particles in 1000 mol; $kmol^{-1}$)
R	universal gas constant

Volumes

V_{AQ}	volume of the aqueous phase (m^3)
V_D	volume of the droplets (m^3)
V_P	volume of the particles (m^3)
V_{POL}	volume of the polymer (m^3)
V_R	engaged volume of the polymerizing system in the reactor (m^3)
V_{R0}	initial volume of the polymerizing system in the reactor (m^3)

Physical constants

M_i	molecular weight of monomer i (kg/kmol)
M_j	molecular weight of monomer j (kg/kmol)
ρ_i	density of monomer i (kg/m^3)
ρ_j	density of monomer j (kg/m^3)
ρ_{Pi}	density of monomer i in the polymer (kg/m^3)

Multicriteria optimization

$A_{\sigma i}$	set of criteria defined by $A_{\sigma i} = \{g_{\sigma i}, \ldots, g_{\sigma n}\}$
$C_\mu(u_1, \ldots, u_n)$	Choquet integral
f_1	objective function 1 (monomer conversion)
f_2	objective function 2 (quality in terms of average molecular weight)
f_3	objective function 3 (AMS fraction incorporated in the copolymer)
GEI	overall evaluation index
g_i	criterion i
$\mu(X)$	fuzzy measure defined under X
σ	index permutation $1, \ldots, n$
u_i	utility of criterion i

References

1. Benyahia, B.; Latifi, M. A.; Fonteix, C.; Pla, F.; Nacef, S. Chem Eng Sci 2010, 65, 850.
2. Courcoux, P.; Qannari, E. M.; Melcion, J. P.; Morat, J. Récents Progrès en Génie des Procédés 1995, 36, 41.
3. Azzaro-Pantel, C.; Bernal-Haro, L.; Baudet, P.; Domenech, S.; Pibouleau, L. Comput Chem Eng 1998, 22, 1461.
4. Logothetis, N.; Haigh, A. Qual Reliability Eng Int 1988, 4, 159.
5. Pareto, V. Cours d'Economie Politique; Droz: Geneva, 1964 (Lausanne, F. Rouge et Paris, 1897).
6. Sareen, R.; Gupta, S. K. J Appl Polym Sci 1995, 58, 2357.
7. Garg, S.; Gupta, S. K. Macromol Theory Simul 1999, 8, 46.
8. Bhaskar, V.; Gupta, S. K.; Ray, A. K. AIChE J 2000, 46, 1046.
9. Nayak, A.; Gupta, S. K. Macromol Theory Simul 2004, 13, 73.
10. Raha, S.; Majumdar, S.; Mitra, K. Macromol Theory Simul 2004, 13, 152.
11. Nagrath, D.; Bequette, B. W.; Cramer, S. M.; Messac, A. AIChE J 2005, 51, 511.
12. Dietz, A.; Azzaro-Pantel, C.; Pibouleau, L.; Domenech, S. Comput Chem Eng 2006, 30, 599.
13. Hoffmann, V. H.; Hungerbuhler, K.; McRae, G. J. Ind Eng Chem Res 2001, 40, 4513.
14. Kiss, L. N.; Zaras, K.; Fonteix, C.; Dominique, R. ASOR Bull 2002, 21, 2.
15. Thibault, J.; Taylor, D.; Yanofsky, C.; Lanouette, R.; Fonteix, C.; Zaras, K. Chem Eng Sci 2003, 58, 203.
16. Massebeuf, S.; Fonteix, C.; Hoppe, S.; Pla, F. J Appl Polym Sci 2003, 87, 2383.
17. Muniglia, L.; Kiss, L. N.; Fonteix, C.; Marc, I. Eur J Operational Res 2003, 153, 360.
18. Renaud, J.; Thibault, J.; Lanouette, R.; Kiss, L. N.; Zaras, K.; Fonteix, C. Eur J Operational Res 2007, 177, 1418.
19. Flores, X.; Rodriguez-Roda, I.; Poch, M.; Jimenez, L.; Banares-Alcantara, R. Ind Eng Chem Res 2007, 46, 5600.
20. Camargo, M.; Fonteix, C.; Morel, L. In Ninth IFAC Symposium on Automated Systems Based on Human Skill and Knowledge, 2006, Nancy, France, 2006; p 1.
21. Choquet, G. Ann Inst Fourier 1954, 5, 131.
22. Grabisch, M. Pattern Recognit Lett 1996, 17, 567.
23. Grabisch, M. Eur J Operational Res 1996, 89, 445.
24. Denguir-Rekik, A.; Mauris, G.; Montmain, J. In Proceedings of the Fourth Joint Conference EUSFLAT-LFA, Barcelona, Spain, 2005; p 997.
25. Ginsburger, E.; Fonteix, C.; Massebeuf, S.; Hoppe, S.; Pla, F. H., P.; Swaels, P. Chem Eng Sci 2003, 58, 4493.
26. Harkins, W. D. J Am Chem Soc 1947, 69, 1428.
27. Gilbert, R. G. Emulsion Polymerization: A Mechanistic Approach; Academic: London, 1995.
28. Golubeva, A.; Usmanova, N. F.; Vansheidt, A. A. J Polym Sci 1961, 52, 63.
29. Ugelstad, J.; Hansen, F. K. Rubber Chem Technol 1976, 49, 536.
30. Nomura, M.; Fujita, K. Polym React Eng 1994, 2, 317.
31. Rawlings, J. B.; Ray, W. H. Polym Eng Sci 1988, 28, 237.
32. Hoppe, S.; Schrauwen, C.; Fonteix, C.; Pla, F. Macromol Mater Eng 2005, 290, 384.
33. McCormick, H. W. J Polym Sci 1957, 25, 488.
34. Asua, J. M.; Adams, M. E.; Sudol, E. D. J Appl Polym Sci 1990, 39, 1183.
35. Villermaux, J.; Blavier, L. Chem Eng Sci 1984, 39, 87.
36. Polymer Handbook, 2nd ed.; Brandrup, J.; Immergut, E. H., Eds.; Wiley: New York, 1975.
37. Walter, E.; Pronzato, L. Identification of Parametric Models from expereimental data, communications and control engineering series, Springer: London, 1997.
38. Greenley, R. Z. J Macromol Sci Pure Appl Chem 1980, 14, 445.
39. Martinet, F.; Guillot, J. J Appl Polym Sci 1997, 65, 2297.
40. Fonseca, C. M.; Fleming, P. J. In Control '94. International Conference on Control; Coventry, UK, 1994; p 745.
41. Viennet, R.; Fonteix, C.; Marc, I. Int J Syst Sci 1996, 27, 255.
42. Viennet, R.; Fonteix, C.; Marc, I. In Artificial Evolution; Springer: Berlin, 1996.
43. Halsall-Whitney, H.; Thibault, J. Comput Chem Eng 2006, 30, 1155.
44. Grabisch, M.; Duchêne, J.; Lino, F.; Perny, P. Fuzzy Optimization Decision Making 2002, 1, 287.